Applied and Environmental Microbiology

LeuO and H-NS are part of an expanded regulatory network for ectoine biosynthesis expression

Katherine Boas Lichty, Gwendolyn J. Gregory, E. Fidelma Boyd*

Department of Biological Sciences, University of Delaware, Newark, DE, 19716

Corresponding author*

E. Fidelma Boyd

Department of Biological Sciences

341 Wolf Hall, University of Delaware

Newark, DE 19716

Phone: (302) 831-1088. Fax: (302) 831-2281 Email: fboyd@udel.edu

Keywords: Ectoine biosynthesis regulation, *Vibrio,* LeuO, NhaR, H-NS, ToxR

Abstract

Bacteria accumulate compatible solutes, to maintain cellular turgor pressure when exposed to high salinity. In the marine halophile *Vibrio parahaemolyticus,* the compatible solute ectoine is biosynthesized *de novo*, which is energetically more costly than uptake; therefore, tight regulation is required. To uncover novel regulators of the ectoine biosynthesis *ectABC-aspk* operon, a DNA affinity pulldown of proteins interacting with the *ectABC-aspk* regulatory region was performed. Mass spectrometry analysis identified, amongst others, five regulators: LeuO, NhaR, OmpR, TorR, and the nucleoid associated protein H-NS. To determine their role in ectoine biosynthesis, in-frame non-polar deletions were made for each gene and P_{ectA}-*gfp* promoter reporter assays were performed. P_{ectA}-*gfp* expression was significantly repressed in the Δ*leuO* mutant and significantly induced in the Δ*nhaR* mutant compared to wild type, suggesting positive and negative regulation, respectively. Both Δ*ompR* and Δ*torR* mutants also showed induced expression of P_{ectA}-*gfp*, but not to the same extent as Δ*nhaR*. The Δ*hns* showed no change compared to wild type. To examine whether H-NS interacts with LeuO or NhaR at the ectoine regulatory region, double deletion mutants were created. In a Δ*leuO*/Δ*hns* mutant, P_{ectA}-*gfp* showed reduced expression, but significantly more than Δ*leuO* suggesting H-NS and LeuO interact to regulate ectoine expression. Whereas Δ*nhaR*/Δ*hns* had no additional effect as compared to Δ*nhaR* suggesting NhaR regulation is independent of H-NS. Next, a P_{leuO}-*gfp* reporter analysis was performed in wild type Δ*leuO*, Δ*hns,* Δ*leuO*/Δ*hns* and Δ*toxR,* which encodes ToxR a positive regulator of *leuO*. P_{leuO}-*gfp* showed significantly increased expression in the Δ*leuO*, Δ*hns* and Δ*leuO*/Δ*hns* mutants as compared to wild type, indicating both are repressors of *leuO,* and Δ*toxR* showed reduced expression. Growth pattern analysis of the Δ*leuO,*

Δ*hns,* and Δ*leuO/*Δ*hns* mutants in M9G 6%NaCl all showed growth defects compared to wild type, with Δ*leuO/*Δ*hns* showing the greatest effect. Overall, the data show that NhaR is a negative regulator and LeuO is a positive regulator of ectoine expression and suggest LeuO is an anti-silencer of H-NS.

Importance: Ectoine is a commercially used compatible solute that acts as a biomolecule stabilizer because of its additional role as a chemical chaperone. The *de novo* biosynthesis of ectoine is carried out by approximately 70% of *Vibrionaceae* species many of which are marine halophiles. This study identified LeuO as a positive regulator of ectoine biosynthesis and also showed that similar to enteric species, LeuO is an anti-silencer of the nucleoid associated protein H-NS. NhaR was a negative regulator of ectoine biosynthesis but growth analysis in high salinity showed that LeuO, NhaR and H-NS are required for optimal growth under these conditions. These data indicate that all three regulators also play a wider role in high NaCl tolerance.

Introduction

When bacteria are exposed to high salinity conditions, an efflux of water across the osmotic gradient occurs lowering cellular turgor pressure (1-5). The initial short-term response to osmotic up shock is the uptake of potassium (K+), which is accompanied by glutamate accumulation in Gram-negative bacteria to maintain electro neutrality. This is the short-term strategy because high concentrations of K+ have deleterious effects on cellular processes (1, 2, 6, 7). The long term response to increased osmotic stress is characterized by the uptake or biosynthesis of compatible solutes, which are small organic molecules that provide osmotic protection by helping to maintain the turgor pressure of the cell and can be accumulated to extremely high intracellular concentrations (3, 8, 9).

63 The compatible solute ectoine was initially discovered to provide osmotic protection in
64 anoxygenic phototrophs (10), but subsequent analysis showed that it functions as a compatible
65 solute in numerous Gram-negative and Gram-positive bacteria (reviewed in (3, 8, 11-14), which
66 included many members of the family *Vibrionaceae* (15-19). The ability to be accumulated to
67 very high intracellular concentrations without interfering with molecular processes is a hallmark
68 of compatible solutes. Additionally, ectoine was shown to act as a chemical chaperone through
69 the stabilization of proteins, thus it is an important compound for commercial uses in medicine
70 and cosmetics to stabilize biomolecules against factors such as heating, freezing, desiccation, and
71 UV radiation (20-23). Therefore, understanding the regulation of the ectoine biosynthetic
72 pathway is important to increase efficient industrial production using natural bacterial producers
73 (24).

74 Biosynthesis of ectoine (1,4,5,6-tetrahydro-2-methyl-4-pyrimidinecarboxylic acid) is *de novo*
75 from L-aspartic acid, and performed by the evolutionarily conserved operon *ectABC,* which
76 encodes the EctA, EctB, and EctC proteins (25-27). In many species an aspartokinase (*aspk*) is
77 clustered with the ectoine biosynthesis operon, which converts aspartic acid to β-aspartyl
78 phosphate, which is then converted to L-aspartate-β-semialdehyde by aspartate semialdehyde
79 dehydrogenase (Asd). This intermediate from the aspartic acid pathway is incorporated into the
80 ectoine biosynthesis pathway when it is converted to L-2,4-diaminobutyrate by EctB (L-2,4-
81 diaminobutyrate transaminase). EctA (L-2,4-diaminobutyrate N^{γ}-acetyltransferase) then
82 acetylates this product to form N^{γ}-acetyldiaminobutyrate. The final step to produce ectoine is a
83 cyclic condensation reaction performed by EctC (L-ectoine synthase) (13, 27).

84 In some species clustered with the ectoine biosynthesis operon is *ectR*, a MarR-type regulator
85 shown to repress transcription of the ectoine operon (24, 28-30). Among *Vibrionaceae*, an *ectR*

86 homolog is only present only in *Aliivibrio* species (31, 32). Previous studies in *V.*
87 *parahaemolyticus* and *V. cholerae* showed that *ectABC-aspK* transcription was repressed in low
88 salinity by another MarR-type regulator named CosR (17, 31, 33). CosR from *V.*
89 *parahaemolyticus* showed 31% amino acid identity to *Aliivibrio fischeri* EctR, with less than
90 60% query coverage and does not cluster with *ectABC-aspk*, but is located elsewhere in the
91 genome (31). The quorum sensing master regulators AphA and OpaR were found to activate and
92 repress expression of *ectABC-aspk*, respectively in *V. parahaemolyticus* (17). AphA and OpaR
93 also regulate expression of CosR, creating a tightly controlled feed-forward loop for ectoine
94 expression across the growth curve (17).

95 In this study, we set out to identify novel regulators of the ectoine biosynthesis genes by
96 performing a DNA affinity chromatography pulldown using the regulatory region of the *ectABC-*
97 *aspk* operon. We identified numerous candidates and selected the regulators LeuO, NhaR,
98 OmpR, TorR, and the nucleoid associated protein (NAP) H-NS to examine further. We
99 constructed in-frame nonpolar deletions in each gene. To determine the role that these putative
100 regulators play, reporter assays were used with *gfp* placed under the control of the regulatory
101 region of the ectoine biosynthesis genes. P_{ectA}-*gfp* expression was first examined in wild type and
102 each single mutant of Δ*leuO,* Δ*nhaR,* Δ*ompR,* Δ*torR,* and Δ*hns*. In addition, double mutants
103 Δ*leuO/*Δ*hns* and Δ*nhaR/*Δ*hns* were constructed to determine whether the NAP, H-NS interacted
104 with either LeuO or NhaR to control ectoine gene expression. To determine the physiological
105 role of LeuO, NhaR and H-NS, growth pattern analysis was performed under high salinity
106 conditions.

107 **Results**

108 **Ectoine is present in cells grown in M9G 3%NaCl and absent in M9G 1%NaCl.** To confirm
109 *V. parahaemolyticus de novo* ectoine biosynthesis is a response to increased salinity, ^{1}H nuclear
110 magnetic resonance spectroscopy (^{1}H-NMR) was performed. Ethanol extracts of *V.*
111 *parahaemolyticus* wild type cells grown in minimal medium supplemented with glucose (M9G)
112 with either 1% NaCl or 3% NaCl overnight at 37C were used to obtain H-NMR spectra (**Fig.**
113 **S1A**). Peaks corresponding to the hydrogen atoms of ectoine are labeled and were present in
114 M9G 3% NaCl extracts but were not detectable in M9G 1%NaCl extracts as previously shown
115 (34) (**Fig. S1A**). In addition to intracellular accumulation of ectoine, we also wanted to
116 demonstrate that *ectABC-aspk* expression is increased in M9G 3%NaCl. A transcriptional
117 reporter assay was performed, where *gfp* was placed under the control of the ectoine regulatory
118 region (P_{ectA}-*gfp*). The expression was examined in wild type cells grown in either M9G 1%NaCl
119 or M9G 3%NaCl by measuring the specific fluorescence of P_{ectA}-*gfp* as a cumulative readout of
120 *ectA* transcription (**Fig. S1B**). The observed level of specific fluorescence of P_{ectA}-*gfp* was
121 significantly increased in M9G 3%NaCl (4.0-fold) relative to that of cells grown in M9G
122 1%NaCl (**Fig. S1B**).

123 **Identification of putative regulators of the ectoine biosynthesis operon.** With the knowledge
124 that ectoine is present in cells grown in M9G 3%NaCl, we performed a promoter pulldown under
125 this growth condition. A promoter pulldown was performed using a 5'-biotin tagged DNA
126 fragment of the *ectABC-aspk* regulatory region bound to streptavidin beads. As a negative
127 control DNA probe, the coding region of downstream *ectB* gene was used. To identify novel
128 regulators of ectoine biosynthesis, we grew cells to mid-exponential phase in M9G 3%NaCl and
129 subsequent cell lysate was incubated with DNA probe-coated beads. Bound proteins were then
130 eluted using a stepwise NaCl gradient and separated with SDS-PAGE gel. Bands that were

131 present in the target lanes, but not present in the *ectB* negative control lanes were selected for
132 analysis via mass spectrometry (**Fig. S2**). The proteins identified with mass spectrometry
133 analysis were aligned to the *V. parahaemolyticus* genome and sorted by gene class and ranked by
134 score (**Table 1**). Candidate proteins of interest that belonged to the transcriptional regulator gene
135 class were selected. These candidate proteins are described in Table 1 and include homologs of
136 regulators NhaR (VP0527), OmpR (VP0154), and TorR (VP1032). NhaR and OmpR had
137 previously been shown in *Escherichia coli* to be involved in osmotic stress (35-40). NhaR, a
138 LysR-type transcriptional regulator, shows 62% amino acid homology to NhaR from *E. coli* K-
139 12, OmpR showed 84% amino acid identity and TorR 57% amino acid homology to OmpR and
140 TorR respectively from *E. coli*. NhaR, OmpR, and TorR have not been previously examined in
141 *Vibrio* species. An additional regulator of interest, LeuO (VP0350) was also examined further. In
142 *V. parahaemolyticus,* LeuO is a LysR-type regulator previously described as under the control of
143 ToxRS and negatively regulated by calcium (41, 42). A homolog of the H-NS (histone-like
144 nucleoid structuring) protein was also identified in our pulldown. In *E. coli* and *Salmonella*
145 *enterica* H-NS was shown to be a universal silencer of gene expression (43-48). In addition, an
146 *E. coli* study by Shimada and colleagues identified 140 LeuO-binding sites with over 90% of
147 these sites also showing H-NS binding. Further studies have shown that LeuO plays a significant
148 role as an antagonist of H-NS gene silencing (43, 49, 50). As a proof of concept for the
149 pulldown, LeuO and NhaR proteins were purified, and electrophoretic mobility shift assays
150 (EMSAs) were performed using the regulatory region of *ectABC-aspk* as a DNA probe. In these
151 assays both proteins bound to the DNA probe (**Fig. S3**).

152 **P*ectA-gfp* reporter shows differential expression in Δ*leuO*, Δ*nhaR*, Δ*ompR* and Δ*torR***
153 **mutants**. To examine the role of *leuO*, *nhaR*, *ompR*, and *torR* candidate regulators in the control

154 of the ectoine biosynthesis operon, we performed GFP reporter assays using a reporter plasmid
155 where *gfp* was under the control of the ectoine regulatory region (P_{ectA}-*gfp*). This reporter
156 plasmid was transformed into wild type or in-frame non-polar mutants of Δ*leuO*, Δ*nhaR*, Δ*ompR*,
157 and Δ*torR*. Cultures were grown overnight in M9G 3%NaCl and relative fluorescence intensity
158 (RFU) was measured. Specific fluorescence was calculated by dividing RFU by OD. From this
159 analysis, the relative fluorescence (RFU) measured in the Δ*leuO* mutant background was 1.7-fold
160 reduced as compared to wild type (**Fig. 1**). This data suggests that LeuO is an activator of ectoine
161 biosynthesis genes. The relative fluorescence measured in a Δ*nhaR* background was significantly
162 increased 1.8-fold as compared to wild type, suggesting that NhaR is a repressor of the ectoine
163 operon (**Fig. 1**). P_{ectA}-*gfp* expression in the Δ*ompR* (1.3-fold) and Δ*torR* (1.4-fold) mutants were
164 also increased as compared to wild type, but not to the same level as NhaR, indicating that both
165 OmpR and TorR are negative regulators of the ectoine biosynthesis operon.

166 **LeuO and H-NS interplay to control P_{ectA}-*gfp*.** In *E. coli* and *V. cholerae*, H-NS has been
167 shown to interact with LeuO in both cooperative and antagonistic relationships at different gene
168 loci (43, 51-54). Therefore, we wanted to examine whether H-NS and LeuO interact at the
169 *ectABC-aspk* locus. We constructed an in-frame non-polar Δ*hns* mutant and a double
170 Δ*leuO*/Δ*hns* mutant to examine H-NS regulation of *ectABC-aspk* in a P_{ectA}-*gfp* reporter assay. In
171 these assays, P_{ectA}-*gfp* in the Δ*leuO* mutant showed significantly reduced expression, and in the
172 Δ*hns* mutant expression was similar to wild type (**Fig. 2**). However, in the Δ*leuO*/Δ*hns* mutant
173 expression was reduced, but not to the same level as the Δ*leuO* single mutant (**Fig. 2**). This
174 indicates interplay between both LeuO and H-NS to control ectoine gene expression with LeuO
175 playing an anti-silencer role.

176 To further investigate the relationship between LeuO and H-NS in *V. parahaemolyticus*, a *gfp*-
177 expressing reporter plasmid under the control of the LeuO regulatory region (P_{leuO}-*gfp*) was
178 constructed. Relative fluorescence and OD_{595} were measured after overnight growth in M9G
179 3%NaCl in wild type, Δ*leuO,* Δ*hns,* Δ*leuO*/Δ*hns,* and Δ*toxR*. When compared to wild type, P_{leuO}-
180 *gfp* expression in the Δ*hns* mutant showed a 4.0-fold increased relative fluorescence indicating
181 that H-NS is a repressor of *leuO* expression (**Fig. 3**). P_{leuO}-*gfp* expression was 2.4-fold higher in
182 Δ*leuO* and 2.8-fold higher in Δ*leuO*/Δ*hns* when compared to wild type. These data indicate that
183 both H-NS and LeuO are repressors of *leuO* expression and in the absence of both negative
184 regulators other proteins are able to access the regulatory region (**Fig. 3**). In *V.*
185 *parahaemolyticus,* ToxR was shown to be a positive regulator of *leuO* expression (41, 55, 56)
186 and this was confirmed in this reporter assay, with Δ*toxRS* (1.8-fold) showing significantly less
187 expression of P_{leuO}-*gfp* when compared to wild type (**Fig. 3**).

188 **H-NS and LeuO are important for growth in high salinity.** To assess whether the deletions of
189 *leuO* and *hns* have a physiological effect, we examined the ability of *V. parahaemolyticus* wild
190 type, Δ*leuO,* Δ*hns,* and Δ*leuO*/Δ*hns* mutants to grow in M9G 1% NaCl, 3% NaCl, or 6% NaCl at
191 37°C (**Fig. 4**). In M9G 1%NaCl and 3%NaCl, there were no significant growth defects observed
192 among the strains examined (**Fig. S4A, B**). However, growth in M9G 6%NaCl showed the wild
193 type and Δ*hns* had a 4 h lag phase, the Δ*leuO* mutant had a lag phase of 5 h, and Δ*leuO*/Δ*hns* had
194 a 12 h lag phase (**Fig. 4**). The double deletion mutant had a final OD_{595} of 0.2, which when
195 compared to wild type with final OD of 0.54 was significantly less (**Fig. 4**). These data
196 demonstrate that both LeuO and H-NS play a significant role in the osmotic stress response and
197 are likely required for salinity tolerance outside of ectoine biosynthesis.

198 **NhaR is a negative regulator of the ectoine biosynthesis operon.** Next, we considered NhaR
199 and H-NS interplay in the regulation of *ectABC-ask*. To accomplish this, we examined
200 transcription of the ectoine biosynthesis regulatory region in a Δ*nhaR*/Δ*hns* double mutant. P_{ectA}-
201 *gfp* expression was significantly higher in a Δ*nhaR* mutant (1.8-fold) as compared to wild type
202 (24,856 RFU/OD) confirming our previous results that NhaR is a negative regulator (**Fig. 5**).
203 P_{ectA}-*gfp* expression in the Δ*hns* mutant (1.0-fold) was similar to wild type. Expression of P_{ectA}-
204 *gfp* in the Δ*hns*/Δ*nhaR* mutant (1.8-fold) was increased as compared to wild type, but not
205 significantly different from Δ*nha*R, suggesting that there is no interplay between H-NS and
206 NhaR in ectoine expression.

207 Next we examined the effect of deleting *nhaR, hns,* and *hns/nhaR* on growth of *V.*
208 *parahaemolyticus*. Growth of the deletion mutants in M9G 1%NaCl and 3% NaCl was similar to
209 wild type (**Fig. S4C, D**). However, Δ*nhaR,* Δ*hns,* and Δ*hns*/Δ*nhaR* mutants grown in M9G 6%
210 NaCl, reached a final OD_{595} of 0.37, 0.36, and 0.38 respectively as compared to wild type OD_{595}
211 of 0.50 (**Fig. 6**). This growth data indicates that there are some defects when grown in increased
212 salinity for Δ*nhaR* but deletion of *hns* does not contribute further to this defect. This supports the
213 expression data that NhaR and H-NS do not interact to control ectoine expression, but the data
214 does indicate that NhaR is important for high NaCl tolerance.

215 **Discussion**

216 When bacterial cells are exposed to increased salinity, the osmotic pressure of the cell decreases
217 and water escapes from the cell (1-4). To maintain the appropriate turgor pressure, small organic
218 compounds called compatible solutes are accumulated (3, 8, 9, 32). This accumulation occurs
219 either via uptake or biosynthesis and in *V. parahaemolyticus* at least four transporters for the
220 uptake of compatible solutes and two compatible solute biosynthesis operons are present (19,

221 57). The biosynthesis of ectoine and not glycine betaine was previously shown to be essential for
222 *V. parahaemolyticus* survival in high salinity (15). However, the biosynthesis of ectoine is costly
223 as it drains intracellular pools of metabolites such as aspartic acid. Therefore, multiple regulators
224 that provide tight control are needed to manage ectoine biosynthesis (58).

225 In this study, we identified several novel regulators of the ectoine biosynthesis operon (**Fig. 7**).
226 We found that NhaR acted as a repressor of ectoine biosynthesis. However, the Δ*nhaR* mutant
227 had a growth defect when grown under high NaCl conditions. This could be explained by the
228 fact that NhaR is known to regulate genes related to the osmotic stress response outside of
229 ectoine biosynthesis (59-62). In *E. coli*, *nhaR* is present in an operon with *nhaA* which encodes a
230 Na+/H+ antiporter. NhaR was shown to activate transcription of *nhaA*, which is induced in high
231 salt and alkaline pH and is essential for survival under these conditions. It was also suggested
232 that NhaR is a sensor and transducer of Na+ because the presence of Na+ alters the contact
233 points between NhaR and the *nhaA* regulatory region (63). Therefore, our observed growth
234 defect further suggests regulation by NhaR at other loci important for the response to increased
235 salinity. A homolog of *nhaA* is present in *V. parahaemolyticus*, which could explain the growth
236 defect in high salinity for the *V. parahaemolyticus* Δ*nhaR* mutant.

237 Our data established that LeuO is a positive regulator of ectoine biosynthesis gene expression.
238 The subsequent analysis of a double Δ*leuO*/Δ*hns* mutant suggests LeuO also likely plays a role
239 as an anti-silencer of H-NS at this locus. In addition, we found that LeuO and H-NS both act as
240 repressors of *leuO* in *V. parahaemolyticus*. LeuO was first identified as a LysR-type regulator
241 and shown to positively regulate the *leuABCD* leucine synthesis operon in *Salmonella enterica*
242 (64, 65). Subsequently, chromatin-immunoprecipitation-on-chip analysis showed 178 LeuO
243 binding sites in *S. enterica*, indicating its role as a global regulator (66). H-NS was also shown to

244 be a global regulator in this species, silencing the transcription of a large number of horizontally
245 acquired genes. Many of these genes clustered together on the genome within pathogenicity
246 islands, regions that were AT rich and allowed H-NS binding along long sections of DNA (47,
247 67). A similar phenomenon was show in *E. coli* horizontally acquired DNA (48). These data led
248 to the idea that H-NS allows for the uptake of horizontally acquired DNA and insertion into the
249 genome in a relatively benign state (45, 47, 67). In *V. parahaemolyticus*, LeuO was first named
250 CalR as it was regulated by calcium (42). LeuO was subsequently shown to negatively control
251 swarming motility (*lafK*) and type III secretion system-1 (T3SS-1, *exsA*) in *V. parahaemolyticus*
252 (41, 42). LeuO was also shown to be regulated by NaCl and to positively regulate *ompU*, which
253 encodes an outer membrane porin important for acid stress (41). Additionally, the global
254 regulator ToxR was shown to be essential for LeuO expression (41). Also, in *V.*
255 *parahaemolyticus*, LeuO was shown to be an antagonist of H-NS at loci required for type VI
256 secretion system-1 (T6SS-1) expression (68). In *V. cholerae*, H-NS was shown to have many
257 roles in silencing genes expression such as those required for capsule biosynthesis and virulence
258 factors acquired by horizontal gene transfer (69-72). In this species, LeuO was shown to be
259 required for biofilm formation, and LeuO and H-NS were shown to interact at the *vieA* locus (53,
260 68, 73, 74). In addition, in *V. vulnificus* another important human pathogen, ToxR was shown to
261 activate *leuO* expression and LeuO was shown to be an auto-repressor with high levels of LeuO
262 binding (73, 74). HNS was subsequently shown to repress *leuO* by binding to sites that overlap
263 with ToxR and LeuO binding sites (73, 74). In a similar pattern, our data also showed that *leuO*
264 is an auto-repressor and that H-NS represses *leuO*, which is likely using a similar regulatory
265 mechanism to that in *V. vulnificus* (**Fig. 7**). Furthermore, our growth data showed that deletion of
266 either *leuO* or *hns* resulted in defects when grown at high salinity and a double Δ*leuO*/Δ*hns*

267 mutant showed a growth defect that was more pronounced than either of the single mutants. The
268 observed defects in high salinity suggests a larger role for both regulators in the osmotic stress
269 response. The more pronounced growth defect observed for Δ*leuO*/Δ*hns* suggest that these
270 proteins interact at other loci important for responses to increased salinity.

271 **Methods**

272 **Bacterial strains, media and culture conditions**. All strains and plasmids used in this study are
273 listed in Table S2. *V. parahaemolyticus* RIMD2210633, a streptomycin-resistant clinical isolate,
274 was used in this study as the wild-type (WT) strain (75, 76). Unless stated otherwise, *V.*
275 *parahaemolyticus* was grown in either lysogeny broth (LB; Fisher Scientific, Fair Lawn, NJ)
276 with 3% (wt/vol) NaCl (LB 3%) or M9 minimal media (47.8 mM Na_2HPO_4, 22 mM KH_2PO_4,
277 18.7 mM NH_4Cl, 8.6 mM NaCl; Sigma Aldrich) supplemented with 2 mM $MgSO_4$, 0.1 mM
278 $CaCl_2$, 20 mM glucose as the sole carbon source (M9G) and 3% (wt/vol) NaCl at 37°C. *E. coli*
279 strains were grown in either LB supplemented with 1% (wt/vol) NaCl (LB1%) or M9G
280 supplemented with 1% (wt/vol) NaCl. The strain *E. coli* β2155 *λpir* strain is a diaminopimelic
281 acid (DAP) auxotrophic strain and was grown with 0.3 mM DAP (77). All strains were grown at
282 37°C with aeration. Antibiotics were added to growth media at the following concentrations as
283 necessary: ampicillin (Amp), 100 µg/mL; chloramphenicol (Cm), 12.5 µg/mL; tetracycline (Tet),
284 1 µg/mL; kanamycin (Km), 50 µg/mL.

285 **Preparation of cellular extracts and proton nuclear magnetic resonance (^{1}H-NMR)**. Wild-
286 type *V. parahaemolyticus* was grown overnight at 37°C in either M9G 1% NaCl or M9G
287 3%NaCl. Stationary phase cells were then pelleted and washed twice with 1XPBS. Three freeze-
288 thaw cycles were performed with the cell pellets to increase lysis, and the cells were then
289 suspended in 750 µL ethanol. Debris was pelleted by centrifugation, and the ethanol solution was

290 transferred to a clean tube and evaporated under vacuum. Then deuterium oxide (D_2O) was used
291 to resuspend the pellet, and insoluble material was removed by centrifugation. The solution was
292 then transferred to a 5-mm NMR tube for analysis on a Bruker AVANCE 600NMR spectrometer
293 at a proton frequency of 600.13 MHz with a sweep of 12,376 Hz and a relaxation delay of 5 s.
294 Sixteen scans were co-added for each spectrum.

295 **DNA-Affinity Pulldown.** DNA-affinity chromatography pulldown was performed as previously
296 described (78-80). The bait DNA primers were designed to amplify the 323-bp regulatory region
297 of *ectA* (VP1722) with a biotin moiety added to the 5' end. A 327-bp negative-control bait DNA
298 probe was amplified from a coding region of *ectB* (VP1721), which was also labeled with a
299 biotin moiety at the 5' end. Both probes were amplified using Phusion HF polymerase (New
300 England Biolabs) PCR. Ten reactions were completed for each probe and then pooled and
301 purified using an ethanol extraction technique (81). The pulldown was completed twice, once
302 after growth in non-inducing conditions (LB3%) and once after growth in inducing conditions
303 (M9G3%) in an effort to obtain both positive and negative regulators of the ectoine biosynthesis
304 operon. The wild-type strain was grown overnight in LB3%, cells were pelleted and washed two
305 times with 1XPBS and diluted 1:50 into 500 mL of LB3% or M9G3%. The cultures were then
306 grown to an OD_{595} of 0.5, pelleted and stored overnight at -80°C. The pellet was then suspended
307 in 1.5 mL Fast-Break lysis buffer (Promega, Madison, WI) with 1 mM PMSF, 0.5 mM
308 benzamidine, 0.1 µg/mL lysozyme and incubated for 30 min. at room temperature. The cells
309 were then sonicated on ice at 30% pulse amplitude for 15 seconds with 1 min. rest, and this was
310 repeated 5 times. The cell lysate was then clarified by centrifugation for 30 min. at 4°C. The cell
311 lysate was precleared with streptavidin DynaBeads (Thermo Scientific, Waltham, MA) to
312 remove nonspecific protein-bead interactions.

313 Streptavidin M280 DynaBeads (ThermoFisher) were then incubated two times with 10 µg of
314 biotinylated probe for 20 min. The precleared cell lysate was then incubated for 30 min. with the
315 bait-coated beads at room temperature with constant rotation in the presence of 100 µg sheared
316 salmon sperm DNA as a non-specific competitor. This was completed twice with washes in
317 between. Protein candidates were then eluted from the bait DNA-bead complex with a stepwise
318 NaCl gradient (100 mM, 200 mM, 300 mM, 500 mM, 170 mM, and 1 M). Next, 6X SDS and 1
319 mM β-mercaptoethanol (BME) was added to elution samples which were then boiled at 95°C for
320 5 min. Samples were then separated using a 12% SDS-PAGE and visualized using the Pierce
321 Silver Stain Kit (ThermoFisher). The P_{ectA} bait and *ectB* negative control were loaded next to
322 each other in order of increasing NaCl concentrations. Bands that were present in the P_{ectA} bait
323 but not the negative control lanes were excised, de-stained, and digested with trypsin following
324 the standard procedure for mass spectrophotometry preparation with C18 ZipTips (Fisher
325 Scientific, Fair Lawn, NJ). The samples were then analyzed with a Q-exactive Orbitrap mass
326 spectrometer with nano-flow electrospray (Thermo). Proteins were subsequently identified using
327 Proteome Discover 2.1 software.

328 **Protein Purification**. Protein were purified as previous described (82). The full-length genes for
329 *leuO* (VP0350) and *nhaR* (VP0527) were cloned into a pET-28a(+) vector with a C-terminal
330 histidine tag, transformed into *E. coli* Dh5α, purified, and sequenced. These vectors pET*leuO*
331 and pET*nhaR* were then transformed into *E. coli* BL21 (DE3) cells, and expression was induced
332 with 0.5mM IPTG at 0.4 OD_{595} and then cells were grown overnight at 25°C. Cells were then
333 pelleted and resuspended with lysis buffer (50 mM sodium phosphate, 200 mM NaCl, 20 mM
334 imidazole, pH 7.4, 1.0 mM phenylmethanesulfonyl fluoride, 0.5 mM benzamidine) and lysed via
335 sonication. Debris was pelleted, and supernatant applied to an IMAC column packed with HisPur

336 Ni-NTA resin (ThermoFisher) that was equilibrated with column buffer (50 mM sodium
337 phosphate, 200 mM NaCl, 20 mM imidazole, pH 7.4). The column was washed with buffer
338 containing increasing concentrations of imidazole (20mM – 100mM) to remove any
339 contaminants. His-tagged proteins were eluted using 500mM imidazole and then dialyzed
340 overnight at 4°C in sodium phosphate buffer to remove any excess salts. Samples of supernatant
341 and each flow through, wash, and elution were analyzed via SDS-PAGE gel to assess protein
342 purity and verify purification.

343 **Electrophoretic mobility shift assay**. DNA fragments were designed as outlined in Table S3, to
344 encompass the entire region (322 bp) or sections of the ectoine biosynthesis regulatory region
345 (125, 137, 106-bp). The concentration of purified protein (LeuO-His or NhaR-His) was
346 determined using the Bradford Assay, and LeuO (0 to 2.175 uM) or NhaR (0 to 2.175 uM) was
347 incubated for 20 minutes with 30 ng of each DNA fragment in a binding buffer (10 mM Tris [pH
348 7.4 at 4°C], 150 mM KCl, 0.1 mM dithiothreitol, 0.1 mM EDTA [pH 8.0], 5% polyethylene
349 glycol). The reactions were then loaded (10 µL) on a 6% native acrylamide gel (pre-run 200V for
350 2 hours at 4°C) and run for 2 hours at 4°C (200V) in 0.5X TBE running buffer. To visualize, gels
351 were stained in an ethidium bromide bath for 15 minutes.

352 **Mutant strain construction**. In-frame deletion mutants of *nhaR* (VP0527), *torR* (VP1032), and
353 *hns* (VP1133), were designed as previously described via allelic exchange (17). A truncated
354 region of the *nhaR* (15-bp of the 891-bp), *torR* (54-bp of the 714-bp), and *hns* (33-bp of the 408-
355 bp) genes was generated using the primers in Table S3. The truncated products were then ligated
356 with the suicide vector pDS132 using the Gibson assembly protocol and transformed into *E. coli*
357 Dh5α (83, 84). The resulting plasmids pDSΔ*nhaR*, pDSΔ*torR,* and pDSΔ*hns* were purified and
358 transformed into *E. coli* β2155 λ*pir* (diaminopimelic acid auxotroph), followed by conjugation

359 and homologous recombination into the *V. parahaemolyticus* RIMD2210633 genome. Single
360 crossover of the plasmids into the genome were selected for by plating onto chloramphenicol
361 (CM) and screened via PCR for a truncated allele. To induce a double-crossover event, the
362 single-cross strain was grown overnight in the absence of CM, leaving behind either the
363 truncated allele or the wild-type allele. The cultures were spread on 10% sucrose plates, and
364 healthy colonies were screened for double-crossover and gene truncation; colonies that contain
365 the plasmid will appear soupy on the plate due to the presence of the *sacB* selectable marker. In-
366 frame deletions were confirmed with sequencing.

367 An in-frame deletion of *ompR* (VP0154) was created in *V. parahaemolyticus* RIMD2210633
368 through splicing by overlap extension (SOE) PCR and homologous recombination (85). Primers
369 were designed to create a 692-bp truncated allele of *ompR* using the primer pair listed in Table
370 S3. This truncated product was ligated into the cloning vector pJET1.2 with T4 DNA ligase and
371 transformed into *E. coli* Dh5α λ*pir*. The truncated *ompR* allele was then excised from the
372 pJETΔ*ompR* vector using restriction enzymes (SacI, XbaI) and ligated into the suicide vector
373 pDS132. The pDSΔ*ompR* vector was then transformed into *E. coli* β2155 λ*pir* (DAP auxotroph),
374 and the same procedure as described above was completed. Double mutants Δ*leuO*/Δ*hns* and
375 Δ*hns*/Δ*nhaR* were generated by conjugating *E. coli* β2155 λ*pir* + pDS*hns* with *V.*
376 *parahaemolyticus* Δ*leuO* and β2155 λ*pir* + pDS*nhaR* with *V. parahaemolyticus* Δ*hns.* The same
377 procedure as described above was carried out to achieve these double deletions.

378 **Transcriptional GFP-reporter assay**. The reporter construct pRUP$_{ectA}$-*gfp* was created
379 previously using the pRU1064 vector, which contains a promoterless *gfp* cassette, as well as Tet
380 and Amp resistance genes (17, 86). Using *E. coli* β2155 λ*pir* containing pRUP$_{ectA}$-*gfp*, the
381 reporter plasmid was conjugated into each of the *V. parahaemolyticus* mutant strains Δ*leuO,*

382 Δ*nhaR,* Δ*torR,* Δ*ompR,* Δ*hns,* Δ*leuO*/Δ*hns,* and Δ*hns*/Δ*nhaR.* Strains were grown overnight in
383 LB3% with tetracycline. The cultures were then washed two times with 1XPBS, diluted 1:100
384 into M9G3% with tetracycline, and grown for 20 hours. The reporter expression was determined
385 by measuring the relative fluorescence with excitation at 385 nm and emission at 509 nm in
386 black, clear bottomed 96-well microplates on a Tecan Spark microplate reader with Magellan
387 software (Tecan Systems, Inc., San Jose, CA). Specific fluorescence was calculated by dividing
388 the relative fluorescence units (RFU) by the optical density of each well. At least two biological
389 replicates were performed for each experiment. Statistics were completed either with a Student's
390 T-test or ANOVA followed by Tukey-Kramer Post Hoc test, as designated.

391 **ACKNOWLEDGEMENTS**

392 This research was supported by a National Science Foundation grant (award IOS-1656688) to
393 E.F.B. KBL and GJG were funded in part by a University of Delaware graduate fellowship
394 award and KBL in part by a Chemistry-Biology Interface predoctoral training program grant:
395 5T32GM008550.

396

397

398

399 **Figure Legends**

400 **Fig. 1.** Expression of a P_{ectA}-*gfp* transcriptional fusion in wild-type (WT) *V. parahaemolyticus*
401 Δ*leuO,* Δ*nhaR*, Δ*ompR,* and Δ*torR* mutants. Cultures were grown overnight in M9G 3% NaCl
402 and relative fluorescence intensity (RFU) was measured. Specific fluorescence was calculated by
403 dividing RFU by OD. Mean and standard deviation of three biological replicates are shown.
404 Statistics were calculated using a Student's t-test; (*, $P < 0.05$; ***, $P < 0.001$).

405 **Fig. 2**. Expression of a P_{ectA}-*gfp* transcriptional fusion in wild-type (WT) *V. parahaemolyticus*
406 Δ*leuO*, Δ*hns,* and Δ*leuO*/Δ*hns* mutants. Cultures were grown overnight in M9G3% and relative
407 fluorescence intensity (RFU) was measured. Specific fluorescence was calculated by dividing
408 RFU by OD. Mean and standard deviation of three biological replicates are shown. Statistics
409 were calculated using an ANOVA followed by Tukey-Kramer post hoc test; (***, $P < 0.001$).

410 **Fig. 3.** Expression reporter assays of P_{leuO}-*gfp* transcriptional fusion in *V. parahaemolyticus* wild
411 type (WT), Δ*leuO*, Δ*hns,* Δ*leuO*/Δ*hns, and* Δ*toxRS* mutants. Cultures were grown overnight in
412 M9G3% and relative fluorescence intensity (RFU) was measured. Specific fluorescence was
413 calculated by dividing RFU by OD. Mean and standard deviation of two biological replicates are
414 shown. Statistics were calculated using a Student's t-test; (*, $P < 0.05$; **, $P < 0.005$).

415 **Fig. 4**. Growth analysis of Δ*leuO,* Δ*hns* and Δ*leuO*/Δ*hns* mutants in M9G supplemented with
416 6%NaCl. Cells were grown to OD 0.5 in M9G1% and then inoculated into M9G M9G 6%NaCl
417 and growth was measured every hour for 24h at 37°C. Mean and standard deviation of two
418 biological replicates are shown. For all growth curves the area under the curve (AUC) was
419 calculated for each strain and a Student's t-test was performed (*, $P < 0.05$; **, $P < 0.005$; ***, P
420 < 0.001).

421 **Fig. 5.** Expression of a P_{ectA}-*gfp* transcriptional fusion in wild type (WT) *V. parahaemolyticus,*
422 Δ*nhaR,* Δ*hns, and* Δ*hns*/Δ*nhaR* mutants. Cultures were grown overnight in M9G3% and relative
423 fluorescence intensity (RFU) was measured. Specific fluorescence was calculated by dividing
424 RFU by OD. Mean and standard deviation of three biological replicates are shown. Statistics
425 were calculated using an ANOVA followed by Tukey-Kramer post hoc test; (***, $P < 0.001$).

426 **Fig. 6**. Growth analysis of Δ*nhaR,* Δ*hns* and Δ*nhaR*/Δ*hns* mutants in M9G supplemented with
427 6%NaCl. Cells were grown to OD 0.5 in M9G1% and then inoculated into M9G6% NaCl and
428 growth was measured every hour for 24 h at 37°C. Mean and standard deviation of two
429 biological replicates are shown. For all growth curves the area under the curve (AUC) was
430 calculated for each strain and a Student's t-test was performed (**, $P < 0.005$).

431 **Fig. 7**. Model of ectoine biosynthesis gene expression in *V. parahaemolyticus*. Solid arrows
432 represent positive regulation while hammer lines represent negative regulation. Previously it was
433 shown that LeuO is required for OmpU expression, an important component of the acid stress
434 response. Our data now show that the LeuO regulon also contains *ectABC* required for high
435 salinity tolerance.

436 **Supplementary data**

437 **Fig. S1. Ectoine production and P*ectA-gfp* expression induced in M9G3% NaCl A**.^{1}H-NMR
438 spectroscopy of *V. parahaemolyticus* wild type (WT) cell lysate grown in M9G 1%NaCl or M9G
439 3%NaCl. The spectral peaks for ectoine are indicated with arrows, and chemical shifts are
440 expressed in ppm. **B**. Expression of P*ectA-gfp* transcriptional fusion in *V. parahaemolyticus* WT.
441 Cultures were grown overnight in M9G 1%NaCl or M9G 3%NaCl and relative fluorescence
442 intensity (RFU) was measured. Specific fluorescence was calculated by dividing RFU by OD.

443 Mean and standard deviation of two biological replicates are shown. Statistics were calculated
444 using a Student's t-test; (**, $P < 0.005$).

445 **Fig. S2. DNA-affinity pulldown, protein separation with SDS-PAGE.** Proteins that bind to
446 the regulatory region of *ectABC-aspk* were identified with DNA affinity chromatography and
447 mass spectrometry. Shown here are gel pieces that were excised to identify candidate proteins.

448 **Fig. S3. LeuO and NhaR bind to the *ectABC-ask* regulatory region. A.** Region upstream of
449 *ectABC-aspk* operon (P_{ectA}) is presented here both as a large probe (2) and segmented into three
450 smaller probes (1A, 1B, and 1C). **B.** LeuO binds to probe P_{ectA}-2 and to the *leuO* regulatory
451 region. **C.** NhaR binds to the P_{ectA}-*2* regulatory region. **D**. LeuO binds to segmented portions of
452 P_{ectA} probes. **E.** NhaR binds to segmented portions of P_{ectA} probes. EMSA's were performed with
453 30 ng of P_{ectA}-*gfp* probe and purified LeuO or NhaR protein (0 to 2.175 uM) with DNA: protein
454 molar rations of 1:0, 1:1, 1:10, 1:20, and 1:50.

455 **Figure S4. Growth analysis of mutants in 1%NaCl and 3%NaCl. A.** Wild type, Δ*leuO,* Δ*hns,*
456 and Δ*leuO/*Δ*hns* in M9G supplemented with 1%NaCl or **B.** M9G 3%NaCl. **C.** Wild type, Δ*nhaR,*
457 Δ*hns,* and Δ*hns/*Δ*nhaR* in M9G 1%NaCl or **D.** M9G 3%NaCl. Cells were grown to OD 0.5 in
458 M9G1% and then inoculated into M9G 1%NaCl or M9G 3%NaCl and growth was measured
459 every hour for 24 h at 37°C. Mean and standard deviation of two biological replicates are shown.

460

461

462 **Table 1. Candidate proteins identified in DNA protein pulldown assay.**

Accession no.	Locus tag	Function/Predicted Domains	Score	Coverage	# AAs	MW [kDa]
Q87RV7	VP0669	Succinylglutamate/aspartoacyclase	29.64	50.84	356	39.0
Q87K62	VPA0036	N-terminal winged helix	23.07	65.63	288	33.2
Q87SD5	VP0489	Aerobic respiration control protein FexA	17.15	9.66	238	26.9
Q87S97	VP0527	NhaR Na+/H+ (NhaA) antiporter regulator	15.06	38.18	296	33.9
Q87SS2	VP0350	LeuO LysR family	13.64	17.87	319	36.2
Q87HC6	VPA1039	IcmF-related protein, type IV SS	11.73	21.93	1172	133.7
Q87QL6	VP1133	H-NS Nucleoid associated protein	10.40	79.26	135	15.1
Q87JF0	VPA0303	DeoR/GlpR family regulators	9.94	17.89	246	26.9
Q87M65	VP2393	GalR LacI family regulators	7.87	3.31	332	36.2
Q87QW7	VP1032	TorR DNA-binding response regulator	7.74	15.19	237	26.7
Q87FD8	VPA1741	MurR/RpiR family regulator	7.47	4.95	283	30.8
Q87IK0	VPA0606	Putative AraC-type regulator	6.64	11.61	267	29.9
Q87T18	VP0252	CytR LacI family regulator	4.51	9.85	335	36.8
Q87RT5	VP0692	GcvA LysR family regulator	4.12	37.25	306	34.5
Q87MQ9	VP2172	YheO, PAS and HTH domains	3.92	40.87	252	28.2
Q87N99	VP1976	MetR LysR family	3.44	28.38	303	34.1
Q87H16	VPA1149	ABC-transporter, SBP domain	2.41	2.42	414	45.3
Q87JP6	VPA0202	GGDEF family protein	2.36	3.26	337	38.2
Q87QW9	VP1030	PurR purine biosynthesis repressor	2.35	4.19	334	37.7
Q87TB6	VP0154	OmpR Osmolarity response regulator	2.33	3.77	239	27.3
Q87QB4	VP1236	Phosphogluconate repressor HexR	2.33	3.52	284	31.5
Q87FZ8	VPA1522	CrgA LysR family regulator	2.30	3.56	309	34.4
Q87S55	VP0569	PhoB DNA-bindng response regulator	2.20	4.80	229	26.1
Q87M71	VP2387	DeoR family transcriptional regulator	2.15	3.80	263	29.2
Q87J66	VPA0387	LysR family transcriptional regulator	2.09	3.86	311	34.7
Q87P35	VP1683	Hypothetical protein; periplasmic binding	2.01	4.31	325	35.0

463

464 **References**

465 1. Wood J. 1999. Osmosensing by bacteria: signals and membrane-based sensors.
466 Microbiology and molecular biology reviews : MMBR 63.
467 2. Poolman B, Glaasker E. 1998. Regulation of compatible solute accumulation in bacteria.
468 Mol Microbiol 29.
469 3. Galinski EA. 1995. Osmoadaptation in bacteria. Adv Microb Physiol 37:272-328.
470 4. Wood JM. 2011. Bacterial osmoregulation: a paradigm for the study of cellular
471 homeostasis. Annu Rev Microbiol 65:215-38.
472 5. Wood J. 2015. Bacterial responses to osmotic challenges. J Gen Physiol 145.
473 6. Csonka L. 1989. Physiological and genetic responses of bacteria to osmotic stress.
474 Microbiol Rev 53.
475 7. McLaggan D, Naprstek J, Buurman ET, Epstein W. 1994. Interdependence of K+ and
476 glutamate accumulation during osmotic adaptation of *Escherichia coli*. J Biol Chem
477 269:1911-7.
478 8. da Costa M, Santos H, Galinski E. 1998. An overview of the role and diversity of
479 compatible solutes in Bacteria and Archaea. Advan Biochemical
480 engineering/biotechnology 61.
481 9. Galinski EA, Oren A. 1991. Isolation and structure determination of a novel compatible
482 solute from the moderately halophilic purple sulfur bacterium Ectothiorhodospira
483 marismortui. Eur J Biochem 198:593-8.
484 10. Galinski EA, Pfeiffer HP, Trüper HG. 1985. 1,4,5,6-Tetrahydro-2-methyl-4-
485 pyrimidinecarboxylic acid. A novel cyclic amino acid from halophilic phototrophic
486 bacteria of the genus Ectothiorhodospira. Eur J Biochem 149:135-9.

487 11. Kempf B, Bremer E. 1998. Uptake and synthesis of compatible solutes as microbial stress
488 responses to high-osmolality environments. Arch Microbiol 170.
489 12. Severin J, Wohlfarth A, Galinski E. 1992. The predominant role of recently discovered
490 tetrahydropyrimidines for the osmoadaptation of halophilic eubacteria. Microbiol 138.
491 13. Czech L, Hermann L, Stöveken N, Richter AA, Höppner A, Smits SHJ, Heider J, Bremer
492 E. 2018. Role of the Extremolytes Ectoine and Hydroxyectoine as Stress Protectants and
493 Nutrients: Genetics, Phylogenomics, Biochemistry, and Structural Analysis. Genes
494 (Basel) 9.
495 14. Hermann L, Mais CN, Czech L, Smits SHJ, Bange G, Bremer E. 2020. The ups and
496 downs of ectoine: structural enzymology of a major microbial stress protectant and
497 versatile nutrient. Biol Chem 401:1443-1468.
498 15. Ongagna-Yhombi SY, Boyd EF. 2013. Biosynthesis of the osmoprotectant ectoine, but
499 not glycine betaine, is critical for survival of osmotically stressed *Vibrio*
500 *parahaemolyticus* Cells. Appl Environ Microbiol, 79:5038-49,
501 16. Pflughoeft KJ, Kierek K, Watnick PI. 2003. Role of ectoine in *Vibrio cholerae*
502 osmoadaptation. Appl Environ Microbiol 69:5919-27.
503 17. Gregory GJ, Morreale DP, Carpenter MR, Kalburge SS, Boyd EF. 2019. Quorum
504 Sensing Regulators AphA and OpaR Control Expression of the Operon Responsible for
505 Biosynthesis of the Compatible Solute Ectoine. Appl Environ Microbiol 85.
506 18. Gregory GJ, Dutta A, Parashar V, Boyd EF. 2020. Investigations of Dimethylglycine,
507 Glycine Betaine, and Ectoine Uptake by a Betaine-Carnitine-Choline Transporter Family
508 Transporter with Diverse Substrate Specificity in Vibrio Species. J Bacteriol 202.

509 19. Naughton LM, Blumerman SL, Carlberg M, Boyd EF. 2009. Osmoadaptation among
510 Vibrio species and unique genomic features and physiological responses of *Vibrio*
511 *parahaemolyticus*. Appl Environ Microbiol 75:2802-10.
512 20. Graf R, Anzali S, Buenger J, Pfluecker F, Driller H. 2008. The multifunctional role of
513 ectoine as a natural cell protectant. Clin Dermatol 26:326-33.
514 21. Buenger J, Driller H. 2004. Ectoin: an effective natural substance to prevent UVA-
515 induced premature photoaging. Skin Pharmacol Physiol 17:232-7.
516 22. Jebbar M, Talibart R, Gloux K, Bernard T, Blanco C. 1992. Osmoprotection of
517 *Escherichia coli* by ectoine: uptake and accumulation characteristics. J Bacteriol 174.
518 23. Sauer T, Galinski EA. 1998. Bacterial milking: A novel bioprocess for production of
519 compatible solutes. Biotechnol Bioeng 57:306-13.
520 24. Czech L, Poehl S, Hub P, Stöveken N, Bremer E. 2018. Tinkering with Osmotically
521 Controlled Transcription Allows Enhanced Production and Excretion of Ectoine and
522 Hydroxyectoine from a Microbial Cell Factory. Appl Environ Microbiol 84.
523 25. Kuhlmann AU, Bremer E. 2002. Osmotically regulated synthesis of the compatible solute
524 ectoine in *Bacillus pasteurii* and related Bacillus spp. Appl Environ Microbiol 68:772-83.
525 26. Reshetnikov AS, Khmelenina VN, Trotsenko YA. 2006. Characterization of the ectoine
526 biosynthesis genes of haloalkalotolerant obligate methanotroph "*Methylomicrobium*
527 *alcaliphilum* 20Z". Arch Microbiol 184:286-97.
528 27. Louis P, Galinski EA. 1997. Characterization of genes for the biosynthesis of the
529 compatible solute ectoine from Marinococcus halophilus and osmoregulated expression
530 in *Escherichia coli*. Microbiology (Reading) 143 (Pt 4):1141-1149.

531 28. Mustakhimov, II, Reshetnikov AS, Fedorov DN, Khmelenina VN, Trotsenko YA. 2012.
532 Role of EctR as transcriptional regulator of ectoine biosynthesis genes in *Methylophaga*
533 *thalassica*. Biochemistry (Mosc) 77:857-63.
534 29. Mustakhimov, II, Reshetnikov AS, Khmelenina VN, Trotsenko YA. 2009. EctR--a novel
535 transcriptional regulator of ectoine biosynthesis genes in the haloalcaliphilic
536 methylotrophic bacterium *Methylophaga alcalica*. Dokl Biochem Biophys 429:305-8.
537 30. Mustakhimov, II, Reshetnikov AS, Glukhov AS, Khmelenina VN, Kalyuzhnaya MG,
538 Trotsenko YA. 2010. Identification and characterization of EctR1, a new transcriptional
539 regulator of the ectoine biosynthesis genes in the halotolerant methanotroph
540 *Methylomicrobium alcaliphilum* 20Z. J Bacteriol 192:410-7.
541 31. Gregory GJ, Morreale DP, Boyd EF. 2020. CosR i a global regulator of the osmotic stress
542 response with widespread distribution among Bacteria. Appl Environ Microbiol 86.
543 32. Gregory GJ, Boyd EF. 2021. Stressed out: Bacterial response to high salinity using
544 compatible solute biosynthesis and uptake systems, lessons from *Vibrionaceae*. Comput
545 Struct Biotechnol J 19:1014-1027.
546 33. Shikuma NJ, Davis KR, Fong JN, Yildiz FH. 2013. The transcriptional regulator, CosR,
547 controls compatible solute biosynthesis and transport, motility and biofilm formation in
548 *Vibrio cholerae*. Environ Microbiol 15:1387-99.
549 34. Ongagna-Yhombi SY, Boyd EF. 2013. Biosynthesis of the osmoprotectant ectoine, but
550 not glycine betaine, is critical for survival of osmotically stressed *Vibrio*
551 *parahaemolyticus* cells. Appl Environ Microbiol 79:5038-49.
552 35. Williams SG, Carmel-Harel O, Manning PA. 1998. A functional homolog of *Escherichia*
553 *coli* NhaR in *Vibrio cholerae*. J Bacteriol 180:762-5.

554 36. Rahav-Manor O, Carmel O, Karpel R, Taglicht D, Glaser G, Schuldiner S, Padan E.
555 1992. NhaR, a protein homologous to a family of bacterial regulatory proteins (LysR),
556 regulates nhaA, the sodium proton antiporter gene in *Escherichia coli*. J Biol Chem
557 267:10433-8.
558 37. Król JE. 2018. Regulatory loop between the CsrA system and NhaR, a high salt/high pH
559 regulator. PLoS One 13:e0209554.
560 38. Pratt LA, Hsing W, Gibson KE, Silhavy TJ. 1996. From acids to osmZ: multiple factors
561 influence synthesis of the OmpF and OmpC porins in *Escherichia coli*. Mol Microbiol
562 20:911-7.
563 39. Kenney LJ, Bauer MD, Silhavy TJ. 1995. Phosphorylation-dependent conformational
564 changes in OmpR, an osmoregulatory DNA-binding protein of *Escherichia coli*. Proc
565 Natl Acad Sci U S A 92:8866-70.
566 40. Chakraborty S, Kenney LJ. 2018. A New Role of OmpR in Acid and Osmotic Stress in
567 *Salmonella* and *E. coli*. Front Microbiol 9:2656.
568 41. Whitaker WB, Parent MA, Boyd A, Richards GP, Boyd EF. 2012. The *Vibrio*
569 *parahaemolyticus* ToxRS Regulator Is Required for Stress Tolerance and Colonization in
570 a Novel Orogastric Streptomycin-Induced Adult Murine Model. Infect Immun, 80:1834-
571 45,
572 42. Gode-Potratz CJ, Chodur DM, McCarter LL. 2010. Calcium and iron regulate swarming
573 and type III secretion in *Vibrio parahaemolyticus*. J Bacteriol 192:6025-38.
574 43. Shimada T, Bridier A, Briandet R, Ishihama A. 2011. Novel roles of LeuO in
575 transcription regulation of *E. coli* genome: antagonistic interplay with the universal
576 silencer H-NS. Mol Microbiol 82:378-97.

577 44. Navarre WW, McClelland M, Libby SJ, Fang FC. 2007. Silencing of xenogeneic DNA
578 by H-NS-facilitation of lateral gene transfer in bacteria by a defense system that
579 recognizes foreign DNA. Genes Dev 21:1456-71.
580 45. Dorman CJ. 2004. H-NS: a universal regulator for a dynamic genome. Nat Rev Microbiol
581 2:391-400.
582 46. Dorman CJ. 2007. H-NS, the genome sentinel. Nat Rev Microbiol 5:157-61.
583 47. Lucchini S, Rowley G, Goldberg MD, Hurd D, Harrison M, Hinton JC. 2006. H-NS
584 mediates the silencing of laterally acquired genes in bacteria. PLoS Pathog 2:e81.
585 48. Oshima T, Ishikawa S, Kurokawa K, Aiba H, Ogasawara N. 2006. *Escherichia coli*
586 histone-like protein H-NS preferentially binds to horizontally acquired DNA in
587 association with RNA polymerase. DNA Res 13:141-53.
588 49. Hernández-Lucas I, Gallego-Hernández AL, Encarnación S, Fernández-Mora M,
589 Martínez-Batallar AG, Salgado H, Oropeza R, Calva E. 2008. The LysR-type
590 transcriptional regulator LeuO controls expression of several genes in *Salmonella*
591 *enterica* serovar Typhi. J Bacteriol 190:1658-70.
592 50. Shimada T, Yamamoto K, Ishihama A. 2009. Involvement of the leucine response
593 transcription factor LeuO in regulation of the genes for sulfa drug efflux. J Bacteriol
594 191:4562-71.
595 51. De la Cruz MA, Fernández-Mora M, Guadarrama C, Flores-Valdez MA, Bustamante
596 VH, Vázquez A, Calva E. 2007. LeuO antagonizes H-NS and StpA-dependent repression
597 in *Salmonella enterica ompS1*. Mol Microbiol 66:727-43.
598 52. Hernández-Lucas I, Calva E. 2012. The coming of age of the LeuO regulator. Mol
599 Microbiol 85:1026-8.

600 53. Ayala JC, Wang H, Benitez JA, Silva AJ. 2018. Molecular basis for the differential
601 expression of the global regulator VieA in *Vibrio cholerae* biotypes directed by H-NS,
602 LeuO and quorum sensing. Mol Microbiol 107:330-343.
603 54. Medina-Aparicio L, Rebollar-Flores JE, Gallego-Hernández AL, Vázquez A, Olvera L,
604 Gutiérrez-Ríos RM, Calva E, Hernández-Lucas I. 2011. The CRISPR/Cas immune
605 system is an operon regulated by LeuO, H-NS, and leucine-responsive regulatory protein
606 in *Salmonella enterica* serovar Typhi. J Bacteriol 193:2396-407.
607 55. Ante VM, Bina XR, Howard MF, Sayeed S, Taylor DL, Bina JE. 2015. *Vibrio cholerae*
608 leuO Transcription Is Positively Regulated by ToxR and Contributes to Bile Resistance. J
609 Bacteriol 197:3499-510.
610 56. Bina XR, Howard MF, Ante VM, Bina JE. 2016. *Vibrio cholerae* LeuO Links the ToxR
611 Regulon to Expression of Lipid A Remodeling Genes. Infect Immun 84:3161-3171.
612 57. Ongagna-Yhombi SY, McDonald ND, Boyd EF. 2015. Deciphering the role of multiple
613 betaine-carnitine-choline transporters in the Halophile *Vibrio parahaemolyticus*. Appl
614 Environ Microbiol 81:351-63.
615 58. Oren A. 1999. Bioenergetic Aspects of Halophilism. doi:10.1128/MMBR.63.2.334-
616 348.1999.
617 59. Dover N, Higgins CF, Carmel O, Rimon A, Pinner E, Padan E. 1996. Na+-induced
618 transcription of nhaA, which encodes an Na+/H+ antiporter in *Escherichia coli*, is
619 positively regulated by nhaR and affected by hns. J Bacteriol 178:6508-17.
620 60. Dover N, Padan E. 2001. Transcription of nhaA, the main Na(+)/H(+) antiporter of
621 *Escherichia coli*, is regulated by Na(+) and growth phase. J Bacteriol 183:644-53.

622 61. Padan E, Gerchman Y, Rimon A, Rothman A, Dover N, Carmel-Harel O. 1999. The
623 molecular mechanism of regulation of the NhaA Na+/H+ antiporter of *Escherichia coli*, a
624 key transporter in the adaptation to Na+ and H+. Novartis Found Symp 221:183-96;
625 discussion 196-9.
626 62. Toesca I, Perard C, Bouvier J, Gutierrez C, Conter A. 2001. The transcriptional activator
627 NhaR is responsible for the osmotic induction of osmC(p1), a promoter of the stress-
628 inducible gene osmC in *Escherichia coli*. Microbiology (Reading) 147:2795-2803.
629 63. Carmel O, Rahav-Manor O, Dover N, Shaanan B, Padan E. 1997. The Na+-specific
630 interaction between the LysR-type regulator, NhaR, and the nhaA gene encoding the
631 Na+/H+ antiporter of *Escherichia coli*. Embo j 16:5922-9.
632 64. Fang M, Majumder A, Tsai KJ, Wu HY. 2000. ppGpp-dependent leuO expression in
633 bacteria under stress. Biochem Biophys Res Commun 276:64-70.
634 65. Hertzberg KM, Gemmill R, Jones J, Calvo JM. 1980. Cloning of an EcoRI-generated
635 fragment of the leucine operon of Salmonella typhimurium. Gene 8:135-52.
636 66. Dillon SC, Espinosa E, Hokamp K, Ussery DW, Casadesús J, Dorman CJ. 2012. LeuO is
637 a global regulator of gene expression in Salmonella enterica serovar Typhimurium. Mol
638 Microbiol 85:1072-89.
639 67. Navarre WW, Porwollik S, Wang Y, McClelland M, Rosen H, Libby SJ, Fang FC. 2006.
640 Selective silencing of foreign DNA with low GC content by the H-NS protein in
641 Salmonella. Science 313:236-8.
642 68. Zhang L, Osei-Adjei G, Zhang Y, Gao H, Yang W, Zhou D, Huang X, Yang H. 2017.
643 CalR is required for the expression of T6SS2 and the adhesion of *Vibrio*
644 *parahaemolyticus* to HeLa cells. Arch Microbiol 199:931-938.

645 69. Yu RR, DiRita VJ. 2002. Regulation of gene expression in *Vibrio cholerae* by ToxT
646 involves both antirepression and RNA polymerase stimulation. Mol Microbiol 43:119-34.
647 70. Stonehouse EA, Hulbert RR, Nye MB, Skorupski K, Taylor RK. 2011. H-NS binding and
648 repression of the ctx promoter in *Vibrio cholerae*. J Bacteriol 193:979-88.
649 71. Ayala JC, Wang H, Benitez JA, Silva AJ. 2015. RNA-Seq analysis and whole genome
650 DNA-binding profile of the *Vibrio cholerae* histone-like nucleoid structuring protein (H-
651 NS). Genom Data 5:147-150.
652 72. Kazi MI, Conrado AR, Mey AR, Payne SM, Davies BW. 2016. ToxR Antagonizes H-NS
653 Regulation of Horizontally Acquired Genes to Drive Host Colonization. PLoS Pathog
654 12:e1005570.
655 73. Park NY, Lee KW, Kim KS. 2020. H-NS Silences Gene Expression of LeuO, the Master
656 Regulator of the Cyclic(Phe-Pro)-dependent Signal Pathway, in Vibrio vulnificus. J
657 Microbiol Biotechnol 30:830-838.
658 74. Park NY, Kim IH, Wen Y, Lee KW, Lee S, Kim JA, Jung KH, Lee KH, Kim KS. 2019.
659 Multi-Factor Regulation of the Master Modulator LeuO for the Cyclic-(Phe-Pro)
660 Signaling Pathway in Vibrio vulnificus. Sci Rep 9:20135.
661 75. Makino K, Oshima K, Kurokawa K, Yokoyama K, Uda T, Tagomori K, Iijima Y, Najima
662 M, Nakano M, Yamashita A, Kubota Y, Kimura S, Yasunaga T, Honda T, Shinagawa H,
663 Hattori M, Iida T. 2003. Genome sequence of *Vibrio parahaemolyticus*: a pathogenic
664 mechanism distinct from that of V cholerae. Lancet 361:743-9.
665 76. Whitaker WB, Parent MA, Naughton LM, Richards GP, Blumerman SL, Boyd EF. 2010.
666 Modulation of Responses of *Vibrio parahaemolyticus* O3:K6 to pH and Temperature

667 Stresses by Growth at Different Salt Concentrations ▿, p 4720-9, Appl Environ
668 Microbiol, vol 76.
669 77. Dehio C, Meyer M. 1997. Maintenance of broad-host-range incompatibility group P and
670 group Q plasmids and transposition of Tn5 in Bartonella henselae following conjugal
671 plasmid transfer from *Escherichia coli*. J Bacteriol 179:538-40.
672 78. Jutras BL, Verma A, Stevenson B. 2012. Identification of novel DNA-binding proteins
673 using DNA-affinity chromatography/pull down. Curr Protoc Microbiol Chapter
674 1:Unit1F.1.
675 79. Chaparian RR, Olney SG, Hustmyer CM, Rowe-Magnus DA, van Kessel JC. 2016.
676 Integration host factor and LuxR synergistically bind DNA to coactivate quorum-sensing
677 genes in Vibrio harveyi. Mol Microbiol 101:823-40.
678 80. Tague JG, Hong J, Kalburge SS, Boyd EF. 2022. Regulatory Small RNA Qrr2 Is
679 Expressed Independently of Sigma Factor-54 and Can Function as the Sole Qrr Small
680 RNA To Control Quorum Sensing in *Vibrio parahaemolyticus*. J Bacteriol
681 204:e0035021.
682 81. Jutras BL, Liu Z, Brissette CA. 2010. Simultaneous isolation of Ixodidae and bacterial
683 (Borrelia spp.) genomic DNA. Curr Protoc Microbiol Chapter 1:Unit1E.2.
684 82. Tague JG, Regmi A, Gregory GJ, Boyd EF. 2021. Fis Connects Two Sensory Pathways,
685 Quorum Sensing and Surface Sensing, to Control Motility in *Vibrio parahaemolyticus*.
686 Front Microbiol 12:669447.
687 83. Gibson DG. 2011. Enzymatic assembly of overlapping DNA fragments. Methods
688 Enzymol 498:349-61.

689 84. Philippe N, Alcaraz JP, Coursange E, Geiselmann J, Schneider D. 2004. Improvement of
690 pCVD442, a suicide plasmid for gene allele exchange in bacteria. Plasmid 51:246-55.
691 85. Horton RM, Hunt HD, Ho SN, Pullen JK, Pease LR. 1989. Engineering hybrid genes
692 without the use of restriction enzymes: gene splicing by overlap extension. Gene 77:61-8.
693 86. Karunakaran R, Mauchline TH, Hosie AHF, Poole PS. 2005. A family of promoter probe
694 vectors incorporating autofluorescent and chromogenic reporter proteins for studying
695 gene expression in Gram-negative bacteria. Microbiology (Reading) 151:3249-3256.

696

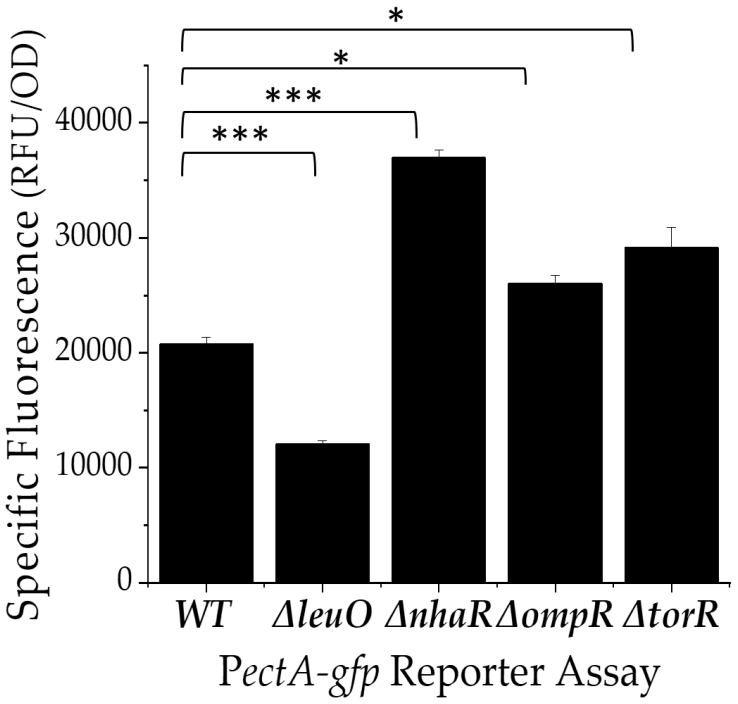
*
*
***
***
Specific Fluorescence (RFU/OD)
40000
30000
20000
10000
0
WT
ΔleuO
ΔnhaR
ΔompR
ΔtorR
PectA-gfp Reporter Assay

Fig. 1

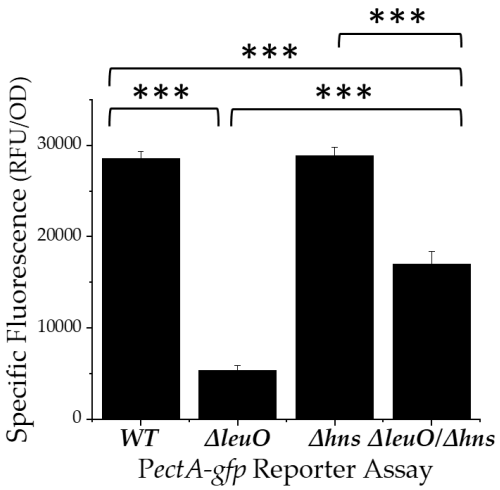
***
***
***
***
Specific Fluorescence (RFU/OD)
30000
20000
10000
0
WT
ΔleuO
Δhns
ΔleuO/Δhns
PectA-gfp Reporter Assay

Fig. 2

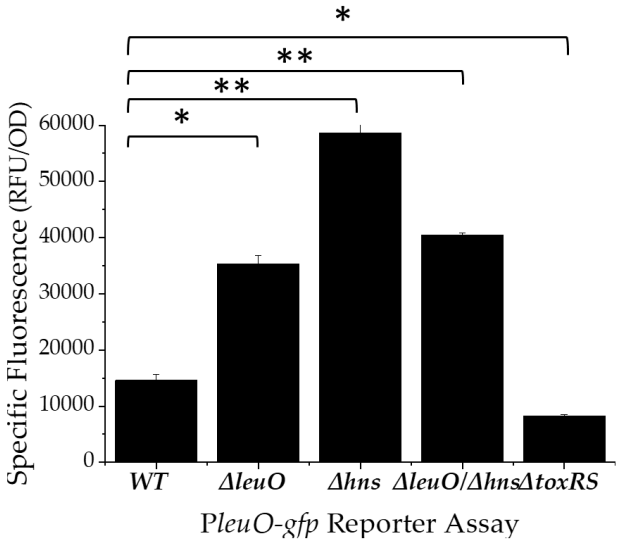
*
**
**
*
Specific Fluorescence (RFU/OD)
60000
50000
40000
30000
20000
10000
0
WT
ΔleuO
Δhns
ΔleuO/Δhns
ΔtoxRS
PleuO-gfp Reporter Assay

Fig. 3

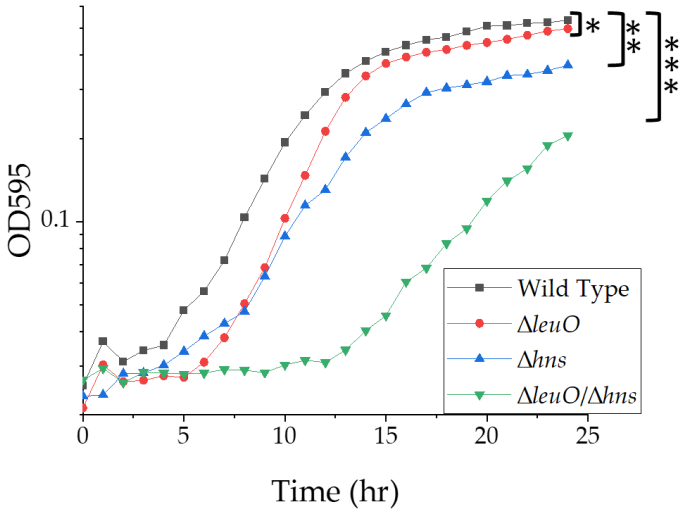

Fig. 4

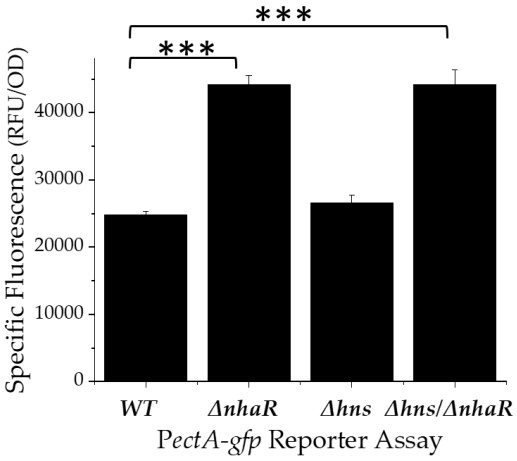
***
***
Specific Fluorescence (RFU/OD)
40000
30000
20000
10000
0
WT
ΔnhaR
Δhns
Δhns/ΔnhaR
PectA-gfp Reporter Assay

Fig. 5

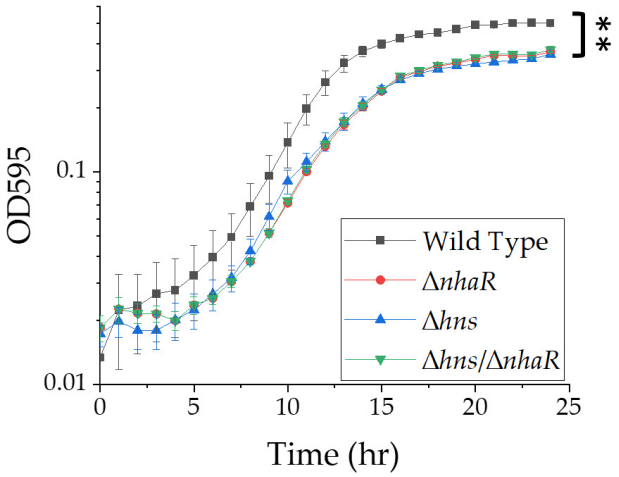
OD595
0.1
0.01
0
5
10
15
20
25
Time (hr)
Wild Type
ΔnhaR
Δhns
Δhns/ΔnhaR
**

Fig. 6

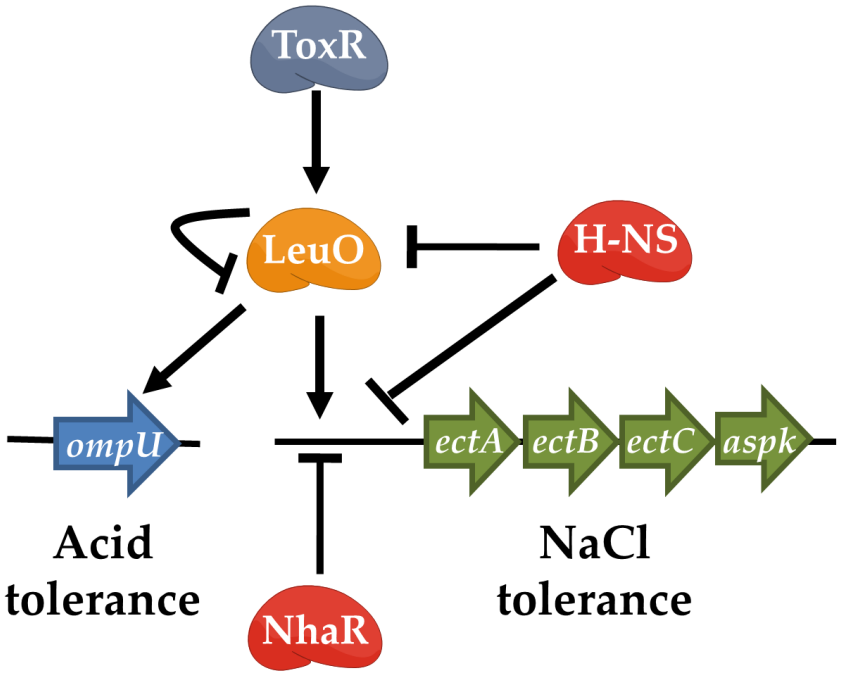
ToxR
LeuO
H-NS
ompU
ectA
ectB
ectC
aspk
Acid
tolerance
NaCl
tolerance
NhaR

Fig. 7